Hindawi Publishing Corporation
International Journal of Antennas and Propagation
Volume 2015, Article ID 181937, 9 pages
http://dx.doi.org/10.1155/2015/181937

Research Article

Design of Fixed Beamformers Based on Vector-Sensor Arrays

Matthew Hawes and Wei Liu

Communications Research Group, Department of Electronic and Electrical Engineering, University of Sheffield, Sheffield S1 3JD, UK

Correspondence should be addressed to Wei Liu; w.liu@sheffield.ac.uk

Received 28 December 2014; Accepted 24 March 2015

Academic Editor: Feifei Gao

Vector-sensor arrays such as those composed of crossed dipole pairs are used as they can account for a signal's polarisation in addition to the usual direction of arrival information, hence allowing expanded capacity of the system. The problem of designing fixed beamformers based on such an array, with a quaternionic signal model, is considered in this paper. Firstly, we consider the problem of designing the weight coefficients for a fixed set of vector-sensor locations. This can be achieved by minimising the sidelobe levels while keeping a unitary response for the main lobe. The second problem is then how to find a sparse set of sensor locations which can be efficiently used to implement a fixed beamformer. We propose solving this problem by converting the traditional l_1 norm minimisation associated with compressive sensing into a modified l_1 norm minimisation which simultaneously minimises all four parts of the quaternionic weight coefficients. Further improvements can be made in terms of sparsity by converting the problem into a series of iteratively solved reweighted minimisations, as well as being able to enforce a minimum spacing between active sensor locations. Design examples are provided to verify the effectiveness of the proposed design methods.

1. Introduction

Traditionally fixed beamformers have been designed assuming the arrays consist of isotropic array elements [1, 2]. As a result the polarisation of a signal is not taken into account when considering the performance of an array. Instead, a vector-sensor array can be considered, allowing measurements of both the horizontal and vertical components of the received waveforms [3–14].

In the past ten years, quaternion-valued signal processing has attracted more and more attention with application areas involving three- or four-dimensional signals [15], and a quaternionic signal model has been introduced into the field of vector-sensor arrays for both adaptive beamforming and direction of arrival (DOA) estimation, [6, 7, 9–11, 13, 16, 17]. A quaternionic formulation provides a compact and convenient representation of three- and four-dimensional signals, although there will not be improvement in performance in theory as equivalent formulations can be established in corresponding domains, that is, two real-valued numbers versus one complex-valued number, or four real-valued numbers (using a "long vector") versus one quaternion-valued number. However, to the best of our knowledge the area of fixed beamformer design for vector-sensor arrays using such a signal model has not been considered yet (in particular, it would be the first time to address the problem of designing sparse vector-sensor arrays).

If such a beamformer is to be implemented using a uniform linear array (ULA), it is well known that the adjacent sensor separation can be no larger than half the operating wavelength, in order to avoid grating lobes. This can be problematic when considering arrays with a large aperture size, due to the cost associated with the number of sensors required. As a result, sparse arrays become a desirable alternative [18], which allow separations to be greater than half a wavelength, while still avoiding grating lobes due to the randomness of sensor locations. However, the tradeoff in using sparse arrays is the unpredictable sidelobe behaviour and it is often necessary to optimise sensor locations in order to achieve a desired performance, (e.g., minimising the peak sidelobe level).

Therefore, the second problem to consider when designing a fixed beamformer is how to find a sparse set of sensor locations that can be efficiently used to implement a desired fixed beamformer. Some nonlinear optimisation methods such as genetic algorithms (GAs) [19–23] and simulated annealing (SA) [24] have been regularly used to achieve

the required location optimisation for sensor arrays. The disadvantage of these methods is the potentially long computation time and the possibility of convergence to a nonoptimal solution.

More recently, the area of compressive sensing (CS) has been explored [25], and CS-based methods have been proposed in the design of sparse arrays [26–32] through l_1 norm minimisation. It is also known that the sparsity of the final array can be improved by converting the problem into a series of iteratively reweighted minimisations [31–35]. This is achieved by the addition of a reweighting term which penalises small weight coefficients more heavily, meaning they are less likely to be repeated in the next iteration. In this paper we propose extending these schemes so that they can be used in designing a sparse set of vector-sensor locations with a quaternionic signal model. This is achieved by reformulating the problem into a modified l_1 norm minimisation similar to what is used for complex-valued minimisation schemes [36] and it can readily be solved using existing convex optimisation toolboxes [37, 38].

A third problem considered in this work is how to enforce a minimum spacing between active locations so that the vector-sensors with a nonzero physical size can fit into the resultant locations in practice. This is an extension of the work in [31], where a size constraint is employed for the design of traditional sparse scalar-sensor arrays.

The rest of this paper is structured as follows: Section 2 gives details of the proposed design method, including some basics about quaternions (Section 2.1), the array model being used (Section 2.2), the method to find the weight coefficients for a fixed set of locations (Section 2.3), the quaternionic CS-based (Section 2.4) and quaternionic reweighted minimisation based (Section 2.5) design methods, and methods of enforcing the size constraint (Section 2.6). Design examples are given in Section 3, with conclusions drawn in Section 4.

2. Proposed Design Method

2.1. Quaternions. A quaternion is a hypercomplex number defined as follows [39]:

$$q = R(q) + iI(q) + jJ(q) + kK(q), \tag{1}$$

where $R(q)$ is the real part of the quaternion and $I(q)$, $J(q)$, and $K(q)$ are the three imaginary components. Similarly for vectors and matrices of quaternions we have

$$\begin{aligned} \mathbf{v} &= R(\mathbf{v}) + iI(\mathbf{v}) + jJ(\mathbf{v}) + kK(\mathbf{v}), \\ \mathbf{M} &= R(\mathbf{M}) + iI(\mathbf{M}) + jJ(\mathbf{M}) + kK(\mathbf{M}). \end{aligned} \tag{2}$$

The conjugate and modulus of a quaternion are given by

$$\begin{aligned} q^* &= R(q) - iI(q) - jJ(q) - kK(q), \\ |q| &= \sqrt{R^2(q) + I^2(q) + J^2(q) + K^2(q)}. \end{aligned} \tag{3}$$

The imaginary units i, j, and k satisfy the following:

$$ii = jj = kk = ijk = -1. \tag{4}$$

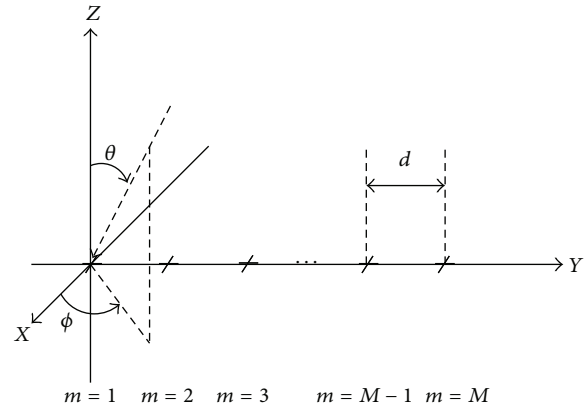

Figure 1: Array model being considered with crossed dipole elements.

Finally $\{\cdot\}^{\triangleleft}$ denotes the conjugate transpose of quaternionic vectors and matrices.

It is worth noting that in many scenarios quaternions prove useful as they allow the easy representation of problems with four-dimensional data. However, care has to be taken when formulating a problem using quaternions as they are noncommutative.

2.2. Quaternionic Array Model. Figure 1 shows the array structure being considered. There are M potentially active crossed dipole pairs located along the y-axis, uniformly spaced a distance d apart. At each location one of the dipoles is parallel to the x-axis and the other to the y-axis. Also shown is a signal with its direction of arrival (DOA) defined by the angles θ and ϕ. Without loss of generality, we assume the signals impinge upon the array from the y-z plane; that is, $\phi = \pi/2$ or $\phi = -\pi/2$. The angle θ is limited to $0 \le \theta \le \pi/2$. A plane-wave signal model is considered; that is, the signal impinges upon the array from the far field.

The spatial steering vector of the array is given by

$$\begin{aligned} \mathbf{s_s}(\theta, \phi) = \Big[1, e^{-j2\pi d \sin\theta \sin\phi/\lambda}, \\ \ldots, e^{-j2\pi(M-1)d \sin\theta \sin\phi/\lambda}\Big]^T, \end{aligned} \tag{5}$$

where λ is the wavelength of the signal of interest and $\{\cdot\}^T$ denotes the transpose operation.

For crossed dipoles the spatial-polarization coherent vector contains information about a signals polarisation and is given by [3–5, 11]

$$\mathbf{s_p}(\theta, \phi, \gamma, \eta) = \begin{cases} \left[-\cos\gamma, \cos\theta \sin\gamma e^{j\eta}\right] & \text{for } \phi = \dfrac{\pi}{2} \\ \left[\cos\gamma, -\cos\theta \sin\gamma e^{j\eta}\right] & \text{for } \phi = -\dfrac{\pi}{2}, \end{cases} \tag{6}$$

where $\gamma \in [0, \pi/2]$ is the auxiliary polarization angle and $\eta \in [-\pi, \pi)$ is the polarization phase difference.

Now the array structure can be split into two subarrays, that is, one parallel to the x-axis and one to y-axis. The steering vector of each of these subarrays is complex-valued and given by

$$\mathbf{s}_{\mathbf{x}}(\theta,\phi,\gamma,\eta) = \begin{cases} -\cos\gamma\mathbf{s}_{\mathbf{s}}(\theta,\phi) & \text{for } \phi = \dfrac{\pi}{2} \\ \cos\gamma\mathbf{s}_{\mathbf{s}}(\theta,\phi) & \text{for } \phi = -\dfrac{\pi}{2}, \end{cases}$$

$$\mathbf{s}_{\mathbf{y}}(\theta,\phi,\gamma,\eta) = \begin{cases} \cos\theta\sin\gamma e^{j\eta}\mathbf{s}_{\mathbf{s}}(\theta,\phi) & \text{for } \phi = \dfrac{\pi}{2} \\ -\cos\theta\sin\gamma e^{j\eta}\mathbf{s}_{\mathbf{s}}(\theta,\phi) & \text{for } \phi = -\dfrac{\pi}{2}. \end{cases} \tag{7}$$

These are then combined to give an overall quaternionic steering vector as follows:

$$\begin{aligned} \mathbf{s}(\theta,\phi,\gamma,\eta) &= \mathbf{s}_{\mathbf{x}}(\theta,\phi,\gamma,\eta) + i\mathbf{s}_{\mathbf{y}}(\theta,\phi,\gamma,\eta), \\ &= R(\mathbf{s}_{\mathbf{x}}(\theta,\phi,\gamma,\eta)) + jJ(\mathbf{s}_{\mathbf{x}}(\theta,\phi,\gamma,\eta)) \\ &\quad + iR\left(\mathbf{s}_{\mathbf{y}}(\theta,\phi,\gamma,\eta)\right) + ijJ\left(\mathbf{s}_{\mathbf{y}}(\theta,\phi,\gamma,\eta)\right), \\ &= R(\mathbf{s}_{\mathbf{x}}(\theta,\phi,\gamma,\eta)) + iR\left(\mathbf{s}_{\mathbf{y}}(\theta,\phi,\gamma,\eta)\right) \\ &\quad + jJ(\mathbf{s}_{\mathbf{x}}(\theta,\phi,\gamma,\eta)) + kJ\left(\mathbf{s}_{\mathbf{y}}(\theta,\phi,\gamma,\eta)\right). \end{aligned} \tag{8}$$

The response of the array is given by

$$P(\theta,\phi,\gamma,\eta) = \mathbf{w}^{\triangleleft}\mathbf{s}(\theta,\phi,\gamma,\eta), \tag{9}$$

where $\mathbf{w}$ is the quaternionic weight coefficient vector defined as

$$\mathbf{w} = \begin{bmatrix} w_1 & w_2 & \cdots & w_M \end{bmatrix}^T, \tag{10}$$

and w_m is a quaternionic value for $m = 1, 2, \ldots, M$.

2.3. Weight Vector Design for a Fixed Set of Locations. The first problem we consider here is that of designing the weight coefficients for a given array geometry, where the sensor locations could be that of a ULA or a known sparse structure or other layouts.

In order to achieve a desirable response (or reference response) $P_r(\theta,\phi,\gamma,\eta)$, we can minimize the error between the designed and desired responses subject to a set of linear constraints to meet any specific requirements of the design, which can be formulated as follows:

$$\begin{aligned} \min_{\mathbf{w}} \quad & \left\|\mathbf{p}_r - \mathbf{w}^{\triangleleft}\mathbf{S}\right\|_2 \\ \text{subject to} \quad & \mathbf{w}^{\triangleleft}\mathbf{S}_C = \mathbf{f}, \end{aligned} \tag{11}$$

where $\|\cdot\|_2$ denotes the l_2 norm,

$$\begin{aligned} \mathbf{p}_r &= \left[P_r(\theta_1,\phi_1,\gamma_1,\eta_1), \ldots, P_r(\theta_L,\phi_L,\gamma_L,\eta_L)\right], \\ \mathbf{S} &= \left[\mathbf{s}(\theta_1,\phi_1,\gamma_1,\eta_1), \ldots, \mathbf{s}(\theta_L,\phi_L,\gamma_L,\eta_L)\right]. \end{aligned} \tag{12}$$

L is the number of points sampled in the desired beam response, $\mathbf{S}_C$ is the constraint matrix, and $\mathbf{f}$ is the corresponding response vector.

In this work, we use the ideal response for $P_r(\theta,\phi,\gamma,\eta)$, that is, a value of one for the main lobe and zeros for the other entries. Here we consider a special case of the above formulation, where we only minimize the design error over the sidelobe region and the designed response is constrained to be unity at the main lobe region. In this case, we have

$$\begin{aligned} \min_{\mathbf{w}} \quad & \left\|\mathbf{p}_r - \mathbf{w}^{\triangleleft}\mathbf{S}\right\|_2 \\ \text{subject to} \quad & \mathbf{w}^{\triangleleft}\mathbf{S}_{ML} = \mathbf{1}, \end{aligned} \tag{13}$$

where $\mathbf{p}_r$ and $\mathbf{S}$ will only cover the sidelobe region, $\mathbf{S}_{ML}$ is constructed in a similar manner to $\mathbf{S}$ but only considers the main lobe of interest, and $\mathbf{1}$ is a vector with a value of unity for all its entries.

To convert the problem into a form that can easily be solved, the quaternionic values have to be split into real and imaginary parts that can be considered separately. This gives the problem in the following form:

$$\begin{aligned} \min_{\widetilde{\mathbf{w}}} \quad & \left\|\widehat{\mathbf{p}}_r - \widetilde{\mathbf{w}}^T\widetilde{\mathbf{S}}\right\|_2 \\ \text{subject to} \quad & R\left(\widetilde{\mathbf{w}}^T\widetilde{\mathbf{S}}_{ML}\right) = \mathbf{1} \\ & I\left(\widetilde{\mathbf{w}}^T\widetilde{\mathbf{S}}_{ML}\right) = \mathbf{0} \\ & J\left(\widetilde{\mathbf{w}}^T\widetilde{\mathbf{S}}_{ML}\right) = \mathbf{0} \\ & K\left(\widetilde{\mathbf{w}}^T\widetilde{\mathbf{S}}_{ML}\right) = \mathbf{0}, \end{aligned} \tag{14}$$

where the following definitions are used:

$$\begin{aligned} \widetilde{\mathbf{w}} &= \left[R(w_1), -I(w_1), -J(w_1), -K(w_1), \ldots,\right. \\ &\qquad \left. R(w_M), -I(w_M), -J(w_M), -K(w_M)\right]^T \\ \widehat{\mathbf{p}}_r &= \left[R(\mathbf{p}_r), I(\mathbf{p}_r), J(\mathbf{p}_r), K(\mathbf{p}_r)\right], \\ \widetilde{\mathbf{S}} &= \begin{pmatrix} R(\mathbf{s}_1) & I(\mathbf{s}_1) & J(\mathbf{s}_1) & K(\mathbf{s}_1) \\ -I(\mathbf{s}_1) & R(\mathbf{s}_1) & -K(\mathbf{s}_1) & J(\mathbf{s}_1) \\ -J(\mathbf{s}_1) & K(\mathbf{s}_1) & R(\mathbf{s}_1) & -I(\mathbf{s}_1) \\ -K(\mathbf{s}_1) & -J(\mathbf{s}_1) & I(\mathbf{s}_1) & R(\mathbf{s}_1) \\ \vdots & \vdots & \vdots & \vdots \\ R(\mathbf{s}_M) & I(\mathbf{s}_M) & J(\mathbf{s}_M) & K(\mathbf{s}_M) \\ -I(\mathbf{s}_M) & R(\mathbf{s}_M) & -K(\mathbf{s}_M) & J(\mathbf{s}_M) \\ -J(\mathbf{s}_M) & K(\mathbf{s}_M) & R(\mathbf{s}_M) & -I(\mathbf{s}_M) \\ -K(\mathbf{s}_M) & -J(\mathbf{s}_M) & I(\mathbf{s}_M) & R(\mathbf{s}_M) \end{pmatrix}, \end{aligned} \tag{15}$$

where $\mathbf{s}_m$ is the mth row vector of the matrix $\mathbf{S}$ and $\widetilde{\mathbf{S}}_{ML}$ is constructed in a similar way to $\widetilde{\mathbf{S}}$ but only using the main lobe.

As mentioned this design method can be used with any known array geometry. However, in many cases, the array geometry is not known in advance and a location optimisation process is needed to find the set of array sensor locations, such as in the sparse array design problem, which will be dealt with in the next subsection.

2.4. CS-Based Design of Sparse Vector-Sensor Arrays. As before, suppose $P_r(\theta, \phi, \gamma, \eta)$ is a reference pattern which we wish to achieve. First, consider Figure 1 as being a grid of potentially active crossed dipole locations. In this instance, $(M-1)d$ is the aperture of the array and M is a large number. Sparseness is then introduced by selecting the weight coefficients to give as few active crossed dipoles as possible, while still giving a designed response that is close to the desired one.

This problem is formulated as

$$\begin{aligned} &\min && \|\mathbf{w}\|_0 \\ &\text{subject to} && \left\|\mathbf{p}_r - \mathbf{w}^{\lhd}\mathbf{S}\right\|_2 \le \alpha, \end{aligned} \tag{16}$$

where $\|\mathbf{w}\|_0$ is the number of nonzero weight coefficients in $\mathbf{w}$, $\mathbf{p}_r$ is the vector holding the desired beam response at the sampled angular and polarisation points of interest, $\mathbf{S}$ is the matrix composed of the corresponding steering vectors, and α places a limit on the allowed difference between the desired and the designed responses.

In practice, (16) is approximated by a minimisation of the l_1 norm of the weight coefficients [25]; that is,

$$\begin{aligned} &\min && \|\mathbf{w}\|_1 \\ &\text{subject to} && \left\|\mathbf{p}_r - \mathbf{w}^{\lhd}\mathbf{S}\right\|_2 \le \alpha. \end{aligned} \tag{17}$$

This formulation is effective for the design of narrowband sparse scalar-sensor arrays. When considering quaternionic coefficients the problem has to be reformulated to ensure the real and three imaginary parts of the quaternion are simultaneously minimised. This is achieved by following a scheme similar to that used when considering the l_1 minimisation of complex data [36]. When all four parts of a quaternionic coefficient are equal to zero, the crossed dipoles can be considered inactive/not present, and as a result sparsity is introduced.

First we rewrite (17) as

$$\begin{aligned} &\min && t \in \mathbb{R}^+ \\ &\text{subject to} && \left\|\mathbf{p}_r - \mathbf{w}^{\lhd}\mathbf{S}\right\|_2 \le \alpha, \quad |\langle \mathbf{w} \rangle|_1 \le t, \end{aligned} \tag{18}$$

where

$$|\langle \mathbf{w} \rangle|_1 = \sum_{m=1}^{M} \left\| \begin{bmatrix} R(w_m) \\ I(w_m) \\ J(w_m) \\ K(w_m) \end{bmatrix} \right\|_2. \tag{19}$$

Now we decompose t to $t = \sum_{m=1}^{M} t_m$, $t_m \in \mathbb{R}^+$. In vector form, we have

$$t = [1, \ldots, 1] \begin{bmatrix} t_1 \\ \vdots \\ t_M \end{bmatrix} = \mathbf{1}^T \mathbf{t}. \tag{20}$$

Then (18) can be rewritten as

$$\begin{aligned} &\min_{\mathbf{t}} && \mathbf{1}^T \mathbf{t} \\ &\text{subject to} && \left\|\mathbf{p}_r - \mathbf{w}^{\lhd}\mathbf{S}\right\|_2 \le \alpha \\ & && \left\| \begin{bmatrix} R(w_m) \\ I(w_m) \\ J(w_m) \\ K(w_m) \end{bmatrix} \right\|_2 \le t_m, \quad m = 1, \ldots, M. \end{aligned} \tag{21}$$

Now define

$$\begin{aligned} \widehat{\mathbf{w}} &= [t_1, R(w_1), -I(w_1), -J(w_1), -K(w_1), \ldots, \\ &\quad R(w_M), -I(w_M), -J(w_M), -K(w_M)]^T \\ \widehat{\mathbf{c}} &= [1, 0, 0, 0, 0, \ldots, 1, 0, 0, 0, 0]^T, \end{aligned}$$

$$\widehat{\mathbf{S}} = \begin{pmatrix} 0 & 0 & 0 & 0 \\ R(\mathbf{s}_1) & I(\mathbf{s}_1) & J(\mathbf{s}_1) & K(\mathbf{s}_1) \\ -I(\mathbf{s}_1) & R(\mathbf{s}_1) & -K(\mathbf{s}_1) & J(\mathbf{s}_1) \\ -J(\mathbf{s}_1) & K(\mathbf{s}_1) & R(\mathbf{s}_1) & -I(\mathbf{s}_1) \\ -K(\mathbf{s}_1) & -J(\mathbf{s}_1) & I(\mathbf{s}_1) & R(\mathbf{s}_1) \\ \vdots & \vdots & \vdots & \vdots \\ 0 & 0 & 0 & 0 \\ R(\mathbf{s}_M) & I(\mathbf{s}_M) & J(\mathbf{s}_M) & K(\mathbf{s}_M) \\ -I(\mathbf{s}_M) & R(\mathbf{s}_M) & -K(\mathbf{s}_M) & J(\mathbf{s}_M) \\ -J(\mathbf{s}_M) & K(\mathbf{s}_M) & R(\mathbf{s}_M) & -I(\mathbf{s}_M) \\ -K(\mathbf{s}_M) & -J(\mathbf{s}_M) & I(\mathbf{s}_M) & R(\mathbf{s}_M) \end{pmatrix}. \tag{22}$$

Finally we arrive at the final formulation for the sparse vector-sensor array design problem

$$\begin{aligned} &\min_{\widehat{\mathbf{w}}} && \widehat{\mathbf{c}}^T \widehat{\mathbf{w}} \\ &\text{subject to} && \left\|\widehat{\mathbf{p}}_r - \widehat{\mathbf{w}}^T \widehat{\mathbf{S}}\right\|_2 \le \alpha \\ & && \left\| \begin{bmatrix} R(w_m) \\ I(w_m) \\ J(w_m) \\ K(w_m) \end{bmatrix} \right\|_2 \le t_m, \quad m = 1, \ldots, M. \end{aligned} \tag{23}$$

2.5. Iteratively Solved Reweighted Quaternionic Minimisations. For the design of sparse arrays consisting of isotropic array elements with real-valued coefficients, reweighted l_1 minimisations are used in order to get a closer approximation to the l_0 minimisation [31, 34, 35]. This is done by solving a series of reweighted l_1 minimisations, where the reweighting term penalises smaller weight coefficients more heavily.

Following the idea, we introduce a reweighting parameter to each quaternionic coefficient. This leads to (23) being altered to

$$\begin{aligned} \min_{\widehat{\mathbf{w}}} \quad & \widehat{\mathbf{c}}^T \widehat{\mathbf{w}} \\ \text{subject to} \quad & \left\| \widehat{\mathbf{p}}_r - \widehat{\mathbf{w}}^T \widehat{\mathbf{S}} \right\|_2 \leq \alpha \\ & a_m^i \left\| \begin{bmatrix} R(w_m) \\ I(w_m) \\ J(w_m) \\ K(w_m) \end{bmatrix} \right\|_2 \leq t_m^i, \\ & m = 0, \ldots, M-1, \end{aligned} \tag{24}$$

where we now have

$$\begin{aligned} \widehat{\mathbf{w}} &= \left[t_1^i, R\left(w_1^i\right), -I\left(w_1^i\right), -J\left(w_1^i\right), -K\left(w_1^i\right), \ldots, \right. \\ &\quad \left. R(w_M^i), -I(w_M^i), -J(w_M^i), -K(w_M^i) \right]^T, \\ \widehat{\mathbf{c}} &= \left[a_0^i, \mathbf{0}_J, a_1^i, \mathbf{0}_J, \ldots, \mathbf{0}_J \right]^T, \\ a_m^i &= \left(\left\| \begin{bmatrix} R(w_m) \\ I(w_m) \\ J(w_m) \\ K(w_m) \end{bmatrix} \right\|_2 + \epsilon \right)^{-1} \end{aligned} \tag{25}$$

with ϵ being set to slightly below the minimum implemented absolute coefficient value for a given location.

The problem is iteratively solved as follows.

(1) Set $i = 1$ and obtain an initial estimate of the weight coefficients by solving (23).

(2) Consider $i = i + 1$; find the reweighting terms a_m^i for all m and solve (24).

(3) Repeat step 2 until the number of active sensor locations has remained constant for three or more iterations of the algorithm.

Note that it is the addition of the reweighting term that improves the sparsity of the solution. If a small nonzero valued combined weight coefficient is found in the previous iteration, it results in a large reweighting term in the current iteration. As a result the nonzero value is unlikely to be repeated, therefore improving the sparsity of the solution. Conversely, a large nonzero valued coefficient will give a small reweighting term. As a result the large nonzero value is likely to be repeated.

2.6. Enforcing the Physical Size Constraint. In above formulations, the solutions do not take the size of the vector-sensors into account. As a result we could end up with an array that could not be implemented in practice due to the vector-sensors not fitting in their deigned locations. Therefore, a minimum spacing of the vector-sensors' physical size should be applied to the optimisation.

This can be achieved using the methods recently proposed in [31], where the postprocessing method and iterative minimum distance sampling method can be directly applied to our sparse vector-sensor array design. These two methods involve some degree of merging locations that are too close together. This is a form of steering vector error that may degrade the performance of the array. As a result, a constraint is required on the minimisation to limit the effects of this error, given by limiting $\varepsilon \|\widetilde{\mathbf{w}}\|_2$ to a small value in the design, where ε is the limit on the expected norm-bounded steering vector error, as normally employed in the design of robust beamformers. To further improve the performance of the array, the weight vector for the final sensor location can be redesigned using the method proposed in Section 2.3.

A third method to enforce the size constraint is to alter the reweighting scheme so that all locations not meeting the size constraint are heavily penalised in order to avoid replication in the next iteration. The modified reweighting terms are given by

$$\delta_m^i = \begin{cases} \left(\left| w_m^{i-1} \right| + \epsilon \right)^{-1} & m = 1 \\ \left(\left| w_m^{i-1} \right| + \epsilon \right)^{-1} & m > 1 \text{ and constraint met} \\ (\epsilon)^{-1} & \text{otherwise.} \end{cases} \tag{26}$$

The iterative procedure detailed in Section 2.5 is now also repeated until a solution complying with the size constraint is met (rather than looking at how many iterations the number of nonzero valued coefficients has remained constant for).

3. Design Examples

In this section design examples will be presented in order to verify the effectiveness of the proposed design methods. This will include one design example based on a ULA and one example to illustrate how the methods can be used to design a sparse vector-sensor array and how the reweighted method can improve the sparsity of the solution. Finally, an example will be given to illustrate the performance of arrays designed while enforcing a size constraint.

For all of the figures that follow, positive values of θ indicate the value range $\theta \in [0^\circ, 90^\circ]$ for $\phi = 90^\circ$, while negative values of $\theta \in [-90^\circ, 0^\circ]$ indicate an equivalent range of $\theta \in [0^\circ, 90^\circ]$ with $\phi = -90^\circ$. The main lobe is designed to be at the single point defined by $\theta = 0^\circ$ and $\phi = 90^\circ$, with the sidelobes given by $\theta = [10^\circ, 90^\circ]$ for $\phi = 90^\circ$ and $\phi = -90^\circ$.

3.1. ULA Based Design Example. First we consider a ULA consisting of ten crossed dipoles with an adjacent separation of 0.5λ. Both here and in all that follows, λ is the wavelength of the signal of interest. The polarisations are given by $(\gamma, \eta) = (30^\circ, 25^\circ)$. By solving (14) to obtain the weight coefficients

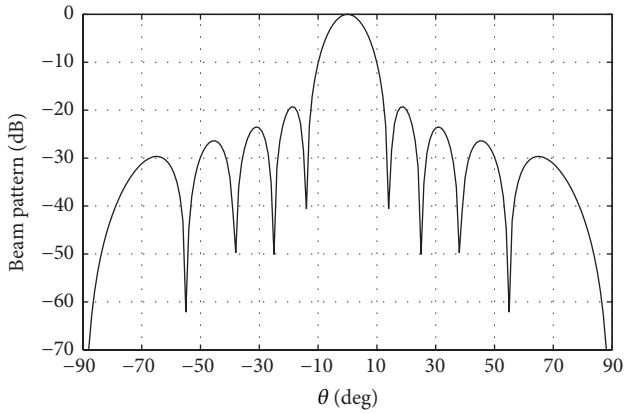

Figure 2: Beam response for the design example based on a ULA.

Table 1: Locations found from solving (23) with a value of $\alpha = 0.94$.

n	d_n/λ	n	d_n/λ	n	d_n/λ
1	4.93	4	6.75	7	8.46
2	5.79	5	7.50	8	9.21
3	6.59	6	8.31	9	10.07

we end up with the response shown in Figure 2. It can be clearly seen that the main lobe is in the correct location and sufficient sidelobe attenuation has been achieved; that is, the minimisation has successfully designed a fixed beamformer.

3.2. Sparse Location Optimisation Design Examples. Now we will consider using the nonreweighted and reweighted minimisations to design sets of sparse locations. In this instance the maximum aperture of the array is 15λ and the polarisation of the signal of interest is defined by $(\gamma, \eta) = (10^\circ, -10^\circ)$.

Firstly, (23) is solved with a value $\alpha = 0.45$. However, this resulted in 44 active locations over an aperture of 13.39λ, giving a mean adjacent sensor separation of 0.31λ. As a result, a ULA of equivalent length could be implemented using a smaller number of crossed dipoles. Therefore, there is no saving in cost and so forth.

By increasing the value of α to 0.94, the designed array instead has 9 active locations over an aperture of 5.13λ, giving a mean adjacent separation of 0.64λ. Therefore, less sensors are required than an equivalent length ULA. On the other hand, as the value of α has been significantly increased there will be more error between the desired and designed responses than the case with $\alpha = 0.45$. The responses for both cases are shown in Figure 3. This clearly shows the degradation in the performance of the array response. The main lobe width has been widened and the sidelobe levels raised. For completeness the locations found for the value of $\alpha = 0.94$ are shown in Table 1.

As an alternative, we can iteratively solve the series of reweighted minimisations given by (24) while using all the original parameters. So there is no increase in the value of α and we still use $\alpha = 0.45$, which suggests there should not be degradation in the performance of the array's response. This

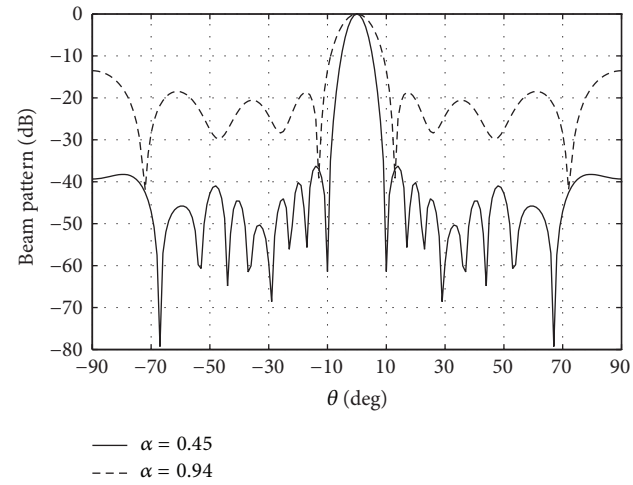

Figure 3: Beam response for the locations found by solving (23).

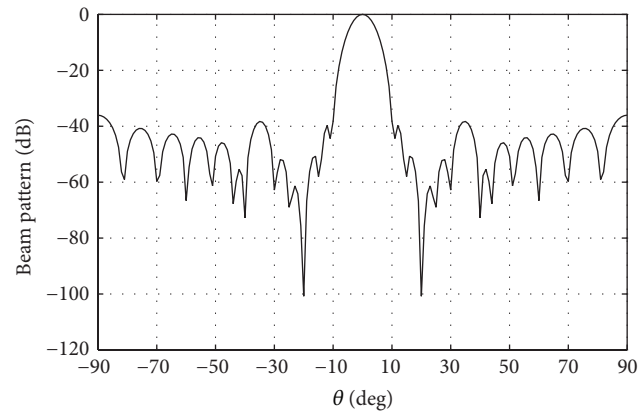

Figure 4: Beam response for the locations found by solving (24).

Table 2: Locations found from solving (24) with a value of $\alpha = 0.45$.

n	d_n/λ	n	d_n/λ	n	d_n/λ
1	2.32	6	6.64	10	10.07
2	3.22	7	7.50	11	10.92
3	4.08	8	8.36	12	11.78
4	4.93	9	9.21	13	12.68
5	5.79				

results in 13 active locations spread over an aperture of 10.37λ as detailed in Table 2. Here the mean adjacent separation is 0.86λ, meaning the array can be implemented with fewer crossed dipoles than a ULA of equivalent length. Figure 4 shows the resulting response and it is clear that an acceptable performance has been achieved.

3.3. Design Examples with Size Constraint. Two examples will now be considered to show the effectiveness of two methods for enforcing the size constraint. For both, the size of the crossed dipoles being considered is assumed to be 0.8λ.

3.3.1. Postprocessing Design Example. For this example we consider an aperture of 15λ split into 300 potential sensor

Table 3: Locations for the postprocessing design example.

n	d_n/λ	n	d_n/λ	n	d_n/λ
1	1.61	6	5.82	11	10.06
2	2.44	7	6.64	12	10.92
3	3.29	8	7.49	13	11.74
4	4.11	9	8.35	14	12.57
5	4.96	10	9.16	15	13.38

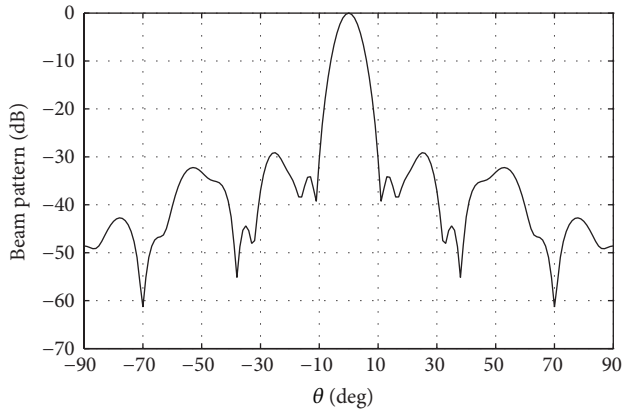

Figure 5: Beam response for the postprocessing design example.

Table 4: Locations for the reweighted design example.

n	d_n/λ	n	d_n/λ	n	d_n/λ
1	2.26	6	6.67	11	10.94
2	3.26	7	7.53	12	11.79
3	4.11	8	8.38	13	12.64
4	4.97	9	9.23	14	13.55
5	5.82	10	10.08		

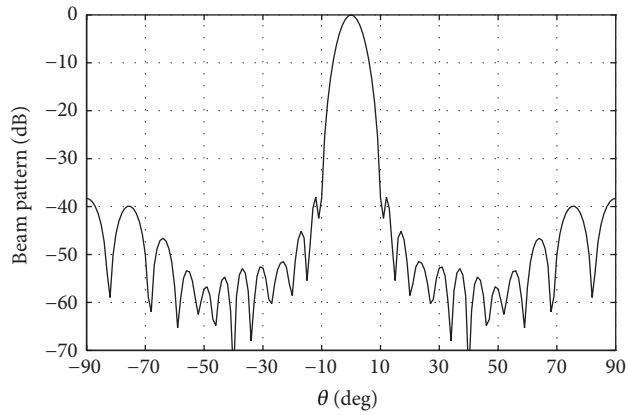

Figure 6: Beam response for the reweighted design example.

locations. In this instance the polarisation of the signal of interest is given by $(\gamma, \eta) = (0^\circ, 0^\circ)$. The values of $\alpha = 0.75$, $\beta = 0.1$, and $\varepsilon = 1$ were used in the constraints placed on the minimisation.

This resulted in 15 crossed dipoles spread over 11.77λ as shown in Table 3. Here the minimum adjacent separation is 0.81λ indicating that the size constraint has been successfully enforced. The resulting response is shown in Figure 5 which shows a desirable response has been achieved.

In order to ensure an acceptable performance here we had to redesign the weight coefficients for the final merged locations. It is reasonable to expect the same from the iterative minimum distance sampling method due to the fact that some merger of location is still required. A similar performance would also be achieved and as a result an example of it is not given here. However, a reweighted design example with size constraint is considered below as an alternative that does not require a redesigning of weight coefficients due to no locations being merged.

3.3.2. Reweighted Design Example. In this example we are now considering 600 possible locations over the same aperture. However, due to the improved sparsity for a given amount of error offered by the reweighted method we can now use a value of $\alpha = 0.3$.

This results in 14 crossed dipole locations shown in Table 4. In this instance the aperture of the designed array is 11.29λ with a minimum adjacent separation of 0.85λ. Again, from Figure 6 we can see that an acceptable response has been achieved.

4. Conclusions

In this paper the problem of designing fixed beamformers based on vector-sensor arrays (with a quaternionic formulation for compact and convenient representation) has been considered. This problem can be split into two parts: first, designing the coefficients for a fixed set of vector-sensor locations and, second, finding a set of sparse locations that can be used to more efficiently implement a fixed beamformer.

The first part of the problem can be solved by minimising the sidelobe levels in the response while keeping a unitary response at the main lobe. For the second part of the problem a reformulation of the traditional l_1 norm minimisation into a modified l_1 norm minimisataion has been proposed. This is required in order to convert the problem into a form that can be solved, while still ensuring that all four parts of the quaternionic weight coefficients are simultaneously minimised. It is also possible to further improve the performance of the proposed method by converting the problem into a series of iteratively reweighted minimisations, as well as enforcing a minimum spacing of the physical size of the sensors being considered. Design examples have been provided to verify the effectiveness of the proposed design methods.

Conflict of Interests

The authors declare that there is no conflict of interests regarding the publication of this paper.

References

[1] H. L. van Trees, *Optimum Array Processing: Part IV of Detection, Estimation, and Modulation Theory*, John Wiley & Sons, New York, NY, USA, 2002.

[2] W. Liu and S. Weiss, *Wideband Beamforming: Concepts and Techniqeus*, John Wiley & Sons, Chichester, UK, 2010.

[3] R. T. Compton Jr., "On the performance of a polarization sensitive adaptive array," *IEEE Transactions on Antennas and Propagation*, vol. 29, no. 5, pp. 718–725, 1981.

[4] J. Li and R. T. Compton Jr., "Angle and polarization estimation using ESPRIT with a polarization sensitive array," *IEEE Transactions on Antennas and Propagation*, vol. 39, no. 9, pp. 1376–1383, 1991.

[5] D. B. Williams and V. Madisetti, Eds., *Digital Signal Processing Handbook*, CRC Press, Boca Raton, Fla, USA, 1st edition, 1997.

[6] S. Miron, N. le Bihan, and J. I. Mars, "High resolution vector-sensor array processing using quaternions," in *Proceedings of the IEEE/SP 13th Workshop on Statistical Signal Processing*, pp. 918–923, July 2005.

[7] S. Miron, N. le Bihan, and J. I. Mars, "Quaternion-music for vector-sensor array processing," *IEEE Transactions on Signal Processing*, vol. 54, no. 4, pp. 1218–1229, 2006.

[8] J.-J. Xiao and A. Nehorai, "Optimal polarized beampattern synthesis using a vector antenna array," *IEEE Transactions on Signal Processing*, vol. 57, no. 2, pp. 576–587, 2009.

[9] X. Gou, Y. Xu, Z. Liu, and X. Gong, "Quaternion-capon beamformer using crossed-dipole arrays," in *Proceedings of the IEEE International Symposium on Microwave, Antenna, Propagation, and EMC Technologies for Wireless Communications (MAPE '11)*, pp. 34–37, November 2011.

[10] J. W. Tao and W. X. Chang, "A novel combined beamformer based on hypercomplex processes," *IEEE Transactions on Aerospace and Electronic Systems*, vol. 49, no. 2, pp. 1276–1289, 2013.

[11] X. R. Zhang, W. Liu, Y. G. Xu, and Z. W. Liu, "Quaternion-valued robust adaptive beamformer for electromagnetic vector-sensor arrays with worst-case constraint," *Signal Processing*, vol. 104, pp. 274–283, 2014.

[12] X. Zhang, Z. Liu, Y. Xu, and W. Liu, "Adaptive tensorial beamformer based on electromagnetic vector-sensor arrays with coherent interferences," *Multidimensional Systems and Signal Processing*, 2014.

[13] J. W. Tao and W. X. Chang, "Adaptive beamforming based on complex quaternion processes," *Mathematical Problems in Engineering*, vol. 2014, Article ID 291249, 10 pages, 2014.

[14] W. Liu, "Antenna array signal processing for a quaternion-valued wireless communication system," in *Proceedings of the Benjamin Franklin Symposium on Microwave and Antenna Subsystems (BenMAS '14)*, Philadelphia, Pa, USA, September 2014.

[15] N. L. Bihan and J. Mars, "Singular value decomposition of quaternion matrices: a new tool for vector-sensor signal processing," *Signal Processing*, vol. 84, no. 7, pp. 1177–1199, 2004.

[16] M. Jiang, W. Liu, and Y. Li, "A general quaternion-valued gradient operator and its applications to computational fluid dynamics and adaptive beamforming," in *Proceedings of the International Conference on Digital Signal Processing (DSP '14)*, pp. 821–826, Hong Kong, August 2014.

[17] M. D. Jiang, Y. Li, and W. Liu, "Properties and applications of a restricted HR gradient operator," http://arxiv.org/abs/1407.5178.

[18] P. Jarske, T. Saramaki, S. K. Mitra, and Y. Neuvo, "On properties and design of nonuniformly spaced linear arrays," *IEEE Transactions on Acoustics, Speech, and Signal Processing*, vol. 36, no. 3, pp. 372–380, 1988.

[19] R. L. Haupt, "Thinned arrays using genetic algorithms," *IEEE Transactions on Antennas and Propagation*, vol. 42, no. 7, pp. 993–999, 1994.

[20] K.-K. Yan and Y. Lu, "Sidelobe reduction in array-pattern synthesis using genetic algorithm," *IEEE Transactions on Antennas and Propagation*, vol. 45, no. 7, pp. 1117–1122, 1997.

[21] K. Chen, Z. He, and C. Han, "Design of 2-dimension sparse arrays using an improved genetic algorithm," in *Proceedings of the 4th IEEE Workshop on Sensor Array and Multichannel Processing*, pp. 209–213, Waltham, Mass, USA, July 2006.

[22] L. Cen, W. Ser, Z. L. Yu, and S. Rahardja, "An improved genetic algorithm for aperiodic array synthesis," in *Proceedings of the IEEE International Conference on Acoustics, Speech and Signal Processing (ICASSP '08)*, pp. 2465–2468, April 2008.

[23] M. B. Hawes and W. Liu, "Location optimization of robust sparse antenna arrays with physical size constraint," *IEEE Antennas and Wireless Propagation Letters*, vol. 11, pp. 1303–1306, 2012.

[24] A. Trucco and V. Murino, "Stochastic optimization of linear sparse arrays," *IEEE Journal of Oceanic Engineering*, vol. 24, no. 3, pp. 291–299, 1999.

[25] E. J. Candes, J. Romberg, and T. Tao, "Robust uncertainty principles: exact signal reconstruction from highly incomplete frequency information," *IEEE Transactions on Information Theory*, vol. 52, no. 2, pp. 489–509, 2006.

[26] L. Li, W. Zhang, and F. Li, "The design of sparse antenna array," http://arxiv.org/abs/0811.0705.

[27] G. Prisco and M. D'Urso, "Exploiting compressive sensing theory in the design of sparse arrays," in *Proceedings of the IEEE Radar Conference*, pp. 865–867, May 2011.

[28] L. Carin, "On the relationship between compressive sensing and random sensor arrays," *IEEE Antennas and Propagation Magazine*, vol. 51, no. 5, pp. 72–81, 2009.

[29] G. Oliveri and A. Massa, "Bayesian compressive sampling for pattern synthesis with maximally sparse non-uniform linear arrays," *IEEE Transactions on Antennas and Propagation*, vol. 59, no. 2, pp. 467–481, 2011.

[30] G. Oliveri, M. Carlin, and A. Massa, "Complex-weight sparse linear array synthesis by Bayesian compressive sampling," *IEEE Transactions on Antennas and Propagation*, vol. 60, no. 5, pp. 2309–2326, 2012.

[31] M. B. Hawes and W. Liu, "Compressive sensing-based approach to the design of linear robust sparse antenna arrays with physical size constraint," *IET Microwaves, Antennas & Propagation*, vol. 8, no. 10, pp. 736–746, 2014.

[32] M. B. Hawes and W. Liu, "Sparse array design for wideband beamforming with reduced complexity in tapped delay-lines," *IEEE/ACM Transactions on Audio, Speech, and Language Processing*, vol. 22, no. 8, pp. 1236–1247, 2014.

[33] E. J. Candes, M. B. Wakin, and S. P. Boyd, "Enhancing sparsity by reweighted l_1 minimization," *Journal of Fourier Analysis and Applications*, vol. 14, no. 5-6, pp. 877–905, 2008.

[34] B. Fuchs, "Synthesis of sparse arrays with focused or shaped beampattern via sequential convex optimizations," *IEEE Transactions on Antennas and Propagation*, vol. 60, no. 7, pp. 3499–3503, 2012.

[35] G. Prisco and M. D'Urso, "Maximally sparse arrays via sequential convex optimizations," *IEEE Antennas and Wireless Propagation Letters*, vol. 11, pp. 192–195, 2012.

[36] S. Winter, H. Sawada, and S. Makino, "On real and complex valued l_1-norm minimization for overcomplete blind source separation," in *Proceedings of the IEEE Workshop on Applications of Signal Processing to Audio and Acoustics*, pp. 86–89, Piscataway, NJ, USA, October 2005.

[37] CVX Research, "CVX: Matlab software for disciplined convex programming," Version 2.0 beta, 2012, http://cvxr.com/cvx.

[38] M. C. Grant and S. P. Boyd, "Graph implementations for nonsmooth convex programs," in *Recent Advances in Learning and Control*, V. Blondel, S. Boyd, and H. Kimura, Eds., vol. 371 of *Lecture Notes in Control and Information Sciences*, pp. 95–110, Springer, Berlin, Germany, 2008.

[39] I. L. Kantor, A. S. Solodovnikov, and A. Shenitzer, *Hypercomplex Numbers: An Elementary Introduction to Algebras*, Springer, New York, NY, USA, 1989.